EUROPEAN ORGANIZATION FOR NUCLEAR RESEARCH (CERN)

CERN-EP-2019-285
LHCb-PAPER-2019-038
December 2, 2020

Constraints on the $K^0_S \to \mu^+\mu^-$ branching fraction

LHCb collaboration[†]

Abstract

A search for the decay $K^0_S \to \mu^+\mu^-$ is performed using proton-proton collision data, corresponding to an integrated luminosity of $5.6\,\text{fb}^{-1}$ and collected with the LHCb experiment during 2016, 2017 and 2018 at a center-of-mass energy of 13 TeV. The observed signal yield is consistent with zero, yielding an upper limit of $\mathcal{B}(K^0_S \to \mu^+\mu^-) < 2.2 \times 10^{-10}$ at 90% CL. The limit reduces to $\mathcal{B}(K^0_S \to \mu^+\mu^-) < 2.1 \times 10^{-10}$ at 90% CL once combined with the result from data taken in 2011 and 2012.

Published in Phys. Rev. Lett. **125**, 231801 (2020)

[†]Authors are listed at the end of this paper.

The decay $K^0_S \to \mu^+\mu^-$ is a flavor-changing neutral current (FCNC) process which has not been observed yet. In the standard model (SM), this decay is highly suppressed [1, 2], with an expected branching fraction $\mathcal{B}(K^0_S \to \mu^+\mu^-)_{\rm SM} = (5.18 \pm 1.50_{\rm LD} \pm 0.02_{\rm SD}) \times 10^{-12}$ [3]. The uncertainties with subscripts LD and SD relate to long-distance and short-distance effects, respectively. The main contributions to the $K^0_S \to \mu^+\mu^-$ decay amplitude are illustrated in Fig. 1. The related channel $K^0_L \to \mu^+\mu^-$ is predicted in the SM to occur with a branching fraction $\mathcal{B}(K^0_L \to \mu^+\mu^-)_{\rm SM} = (6.85 \pm 0.80_{\rm LD} \pm 0.06_{\rm SD}) \times 10^{-9}$ or $\mathcal{B}(K^0_L \to \mu^+\mu^-)_{\rm SM} = (8.11 \pm 1.49_{\rm LD} \pm 0.13_{\rm SD}) \times 10^{-9}$ for an (unknown) positive or a negative relative sign of the $K^0_L \to \gamma\gamma$ amplitude [4], respectively. These predictions are in good agreement with the experimental world average $\mathcal{B}(K^0_L \to \mu^+\mu^-) = (6.84 \pm 0.11) \times 10^{-9}$ [5], based on Refs. [6–8]. Both the K^0_S and the K^0_L decay amplitudes are dominated by LD contributions in the SM. The large difference between the two branching fractions is due to the *S-wave* component, which is charge-parity (*CP*) violating and *CP* conserving for the K^0_S and K^0_L modes, respectively. In the K^0_S case, the *CP*-conserving long-distance contribution can only proceed through the *P-wave*, and the *CP*-violating short distance component in the SM is even more suppressed.

Because of the strong suppression of the SM decay amplitude, dynamics beyond the standard model (BSM) can induce large deviations of $\mathcal{B}(K^0_S \to \mu^+\mu^-)$ with respect to the SM prediction. This has been shown to be the case in SUSY scenarios [9] as well as in leptoquark models [10, 11]. The current best limit, $\mathcal{B}(K^0_S \to \mu^+\mu^-) < 0.8 \times 10^{-9}$ at 90% confidence level (C.L.), was set by LHCb [12] with the data collected during Run 1 (2011–2012).

In this letter, a significantly improved limit is presented. Results are based on proton-proton (*pp*) collision data collected with the LHCb detector at a center-of-mass energy of 13 TeV during 2016, 2017, and 2018 (Run 2), corresponding to an integrated luminosity of $5.6\,\text{fb}^{-1}$. This measurement benefits from the huge K^0_S production cross section at the LHC of approximately 0.6 b at a center-of-mass energy of 13 TeV [13], and from the forward geometry of the vertex detector of LHCb since K^0_S mesons are predominantly produced at low angles with respect to the beam pipe. A major improvement with respect to the previous analysis is achieved by employing dedicated software triggers that were

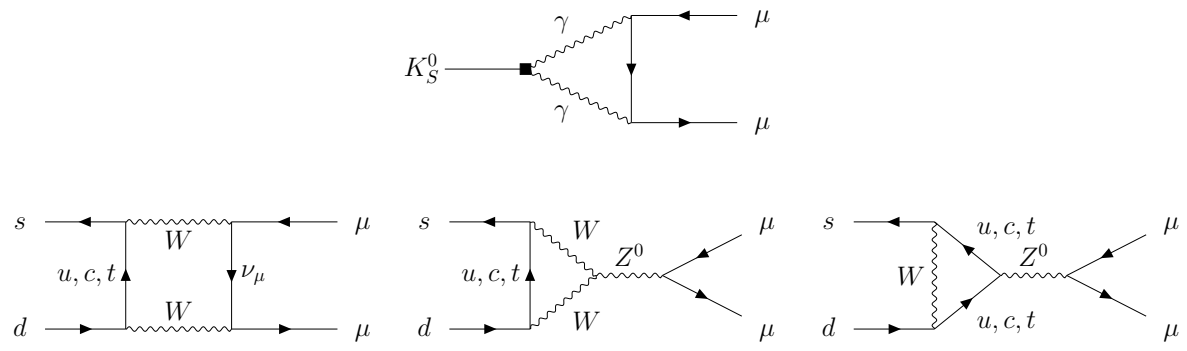

Figure 1: Diagrams representing SM contributions to the $K^0_S \to \mu^+\mu^-$ decay amplitude: (top) long-distance contribution, generated by two intermediate photons, and (bottom) short-distance contributions.

not present in Run 1. These new triggers were included from the start of 2016 data taking, so data from 2015 is not used, due to a lower trigger efficiency and integrated luminosity. While the analysis strategy closely follows what was done for Run 1, the event reconstruction and selection have been improved.

The LHCb detector [14, 15] is a single-arm forward spectrometer covering the pseudorapidity range $2 < \eta < 5$, designed for the study of particles containing b or c quarks. The detector includes a high-precision tracking system consisting of a silicon-strip vertex detector (VELO) surrounding the pp interaction region, a large-area silicon-strip detector located upstream of a dipole magnet with a bending power of about 4 Tm, and three stations of silicon-strip detectors and straw drift tubes placed downstream of the magnet. The tracking system provides a measurement of the momentum, p, of charged particles with a relative uncertainty that varies from 0.5% at low momentum to 1.0% at 200 GeV/c. The minimum distance of a track to a proton-proton collision vertex (PV), the impact parameter (IP), is measured with a resolution of $(15 + 29/p_{\rm T})$ µm, where $p_{\rm T}$ is the component of the momentum transverse to the beam axis, in GeV/c. Different types of charged hadrons are distinguished using information from two ring-imaging Cherenkov (RICH) detectors. Photons, electrons and hadrons are identified by a calorimeter system consisting of scintillating-pad and preshower detectors, an electromagnetic and a hadronic calorimeter. Muons are identified by a system composed of alternating layers of iron and multiwire proportional chambers. In addition, information from the tracking system, the calorimeter system and the RICH detectors is used to further improve the muon identification.

Events are first required to pass a hardware-trigger selection [16], based on information from the calorimeter and the muon system, relying on high-$p_{\rm T}$ signatures. Subsequently, a full event reconstruction is applied in a two-step software selection. In the previous analysis, the search was limited by a muon $p_{\rm T}$ threshold of approximately 1.8 GeV/c. In Run 2, a new tracking method was included, in order to improve the reconstruction of muons with low transverse momentum. By using the information from the muon chambers at early stages in the reconstruction chain, a drastic reduction of the number of tracks to be processed by the most time-consuming reconstruction algorithms is achieved. This new reconstruction method allowed to reduce the $p_{\rm T}$ muon threshold to 80 MeV/c. In addition, a dedicated software trigger selection was developed, using the aforementioned reconstruction method, fully covering the dimuon invariant mass spectra of many strange decays, including $K^0_{\rm S} \to \mu^+\mu^-$. This translates into an increase of the trigger efficiency for $K^0_{\rm S} \to \mu^+\mu^-$ of about an order of magnitude with respect to Run 1 [17]. After the upgrade of the LHCb detector [18], the hardware trigger will no longer be present, allowing for further efficiency improvements.

The purity of the signal candidates and the evaluation of the systematic uncertainties depend on the hardware trigger requirements, so the full data sample is divided into two categories. In the first category, referred to as triggered-independent-of-signal (TIS), events are triggered at the hardware stage independently of the trigger decision on the decay products of the signal candidate. The second category, referred to as exclusively triggered-on-signal (XTOS), consists of events triggered at the hardware stage by the signal candidate decay products that are not contained in the TIS category [19]. Both categories are required to fulfill the same software trigger requirements.

The measurement of the $K^0_{\rm S} \to \mu^+\mu^-$ branching fraction requires the normalization to the $K^0_{\rm S}$ meson production rate, which is done using $K^0_{\rm S} \to \pi^+\pi^-$ decays, given its

abundance, its similar topology to $K^0_S \to \mu^+\mu^-$ and its well-known branching fraction [5]. Common off-line preselection criteria are applied to $K^0_S \to \mu^+\mu^-$ and $K^0_S \to \pi^+\pi^-$ candidates in order to reduce many systematic effects in the efficiency ratio. Candidate $K^0_S \to \mu^+\mu^-$ ($K^0_S \to \pi^+\pi^-$) decays are obtained from two tracks with opposite charge identified as muons (pions), forming a secondary vertex (SV) and with an invariant mass in the range 400–600 MeV/c^2. Kaon candidates are required to decay inside the VELO, where the best K^0_S invariant mass resolution is achieved. Approximately 22% of K^0_S mesons produced at the pp interaction point decay within the acceptance of the VELO. The K^0_S candidate origin must be compatible with a PV, while its decay products should be inconsistent with originating from any PV. The SV must be well detached from the PV by requiring the K^0_S candidate decay time to be larger than 6% of the known K^0_S lifetime [5]. Decays of Λ baryons to $p\pi^-$, and the charge-conjugate counterpart, are suppressed by removing candidates close to the expected elliptical kinematic regions in the Armenteros–Podolanski plane [20] (The inclusion of charge-conjugate processes is implied throughout this paper, unless otherwise noted.). The corresponding loss in signal efficiency is negligible. Muon tracks are required to have associated hits in the muon system [21], while pions from $K^0_S \to \pi^+\pi^-$ decays are required to be within the muon system acceptance. The main background sources are random combinations of tracks, inelastic interactions with the detector material, and $K^0_S \to \pi^+\pi^-$ decays, where the two pions are misidentified as muons. In doubly misidentified $K^0_S \to \pi^+\pi^-$ decays, the invariant mass of the kaon candidate is underestimated on average by 40 MeV/c^2, corresponding to ten times the dimuon invariant mass resolution in this energy regime.

Background from material interactions and random combinations of tracks is suppressed using two adaptive boosted decision tree (BDT) [22, 23] algorithms based on the XGBoost library [24] and optimized for each trigger category. Simulated $K^0_S \to \mu^+\mu^-$ decays are used as a proxy for signal, and $K^0_S \to \mu^+\mu^-$ candidates from data in the dimuon invariant mass region above 520 MeV/c^2 as a proxy for background. Data from the left sideband are not considered since it is dominated by doubly misidentified $K^0_S \to \pi^+\pi^-$ decays. Before the BDT training, the simulated $K^0_S \to \mu^+\mu^-$ candidates are weighted using a gradient boost algorithm [25] trained with $K^0_S \to \pi^+\pi^-$ candidates in simulation and data, to take into account small differences between data and simulation. Since the background candidates used in the training are part of the fitted sample, the *k-folding* approach [26] is applied to maximize the sample available without biasing the background estimate. The BDT input variables are the kaon candidate decay time and IP significance ($\chi^2_{\rm IP}$), defined as the increase of the χ^2 of the PV when considering the kaon candidate in the vertex fit; the $\chi^2_{\rm IP}$ and the track-fit χ^2 of each of the two tracks; the distance of closest approach between the two tracks; the cosine of the helicity angle; the χ^2 of the SV fit; two SV isolation variables, defined as the difference in the χ^2 in the vertex fit with only the two final-state tracks and that obtained when adding the one or two nearest tracks; and a VELO material veto variable [27]. The VELO material veto variable efficiently suppresses background originating from inelastic interactions with the VELO stations and RF foil which separates the VELO modules from the beam vacuum. See Appendix A for more information about the material veto and the interactions with the VELO material. A selection requirement is placed on the BDT, rejecting 99% of the background with a signal efficiency of approximately 63% for both trigger categories.

Another significant background source is $K^0_L \to \mu^+\mu^-$ decays, for which the LHCb detector has the efficiency suppressed by a factor of approximately 2.3×10^{-3} relative to

$K^0_S \to \mu^+\mu^-$ decays due to its longer lifetime. Interference between K^0_S and K^0_L mesons is neglected since K^0 and $\overline{K}^0$ mesons are expected to be produced in equal amounts [3] at the LHC. Contributions from other background sources, such as $K^0 \to \mu^+\mu^-\gamma(\gamma)$, $\Sigma^+ \to p\mu^+\mu^-$, $K^{0,+} \to \pi^{0,+}\mu^+\mu^-$, $\Lambda \to p\pi^-$, $\omega \to \pi^0\mu^+\mu^-$, $\eta \to \mu^+\mu^-\gamma$, as well as from $K^0_L \to \pi^\pm\mu^\mp\nu_\mu$ and $K^0_S \to \pi^\pm\mu^\mp\nu_\mu$ decays, the latter recently discovered by the KLOE-2 Collaboration [28], are found to be negligible.

Candidates satisfying the preselection criteria are divided into twenty subsets: ten bins of the BDT response for each of the two trigger categories. The BDT bins are chosen to have the same fraction of simulated signal candidates in each bin. A dedicated muon identification boosted decision tree (μBDT) is used to suppress $K^0_S \to \pi^+\pi^-$ decays, whose performance can be consulted in Ref. [12]. The selection criterion on the μBDT is optimized and applied independently for each of the twenty categories. The response of the muon identification is calibrated using $J/\psi \to \mu^+\mu^-$ decays, complemented with the use of $K^0 \to \pi^-\mu^+\nu_\mu$ decays due to the lower transverse momentum of the decay products.

The $K^0_S \to \mu^+\mu^-$ branching fraction is determined in an unbinned maximum-likelihood fit to the kaon candidate invariant mass in the range 480–595 MeV/c^2. Taking into account the ratio of detection efficiencies, the signal yield is normalized to $K^0_S \to \pi^+\pi^-$ decays to cancel uncertainties due to the K^0_S cross section, luminosity, reconstruction, and partially due to selection criteria including the BDT binning. The fit is performed simultaneously in the twenty data categories. The contributions considered are $K^0_S \to \mu^+\mu^-$ signal, modelled with a Hypatia distribution [29]; background from material interactions and random combination of tracks, described by an exponential function; the $K^0_S \to \pi^+\pi^-$ background, modelled with a power law distribution; and $K^0_L \to \mu^+\mu^-$, described with the same probability density function as the $K^0_S \to \mu^+\mu^-$ decay. All yields are free to vary in the fit. Because of the low level of background from material interactions and random combination of tracks, the slope of the exponential function is left to change sign when constructing the profile likelihood. A Gaussian constraint is applied to the yield of the $K^0_L \to \mu^+\mu^-$ component, based on its known branching fraction [5] and on the efficiency ratios between $K^0_L \to \mu^+\mu^-$ and $K^0_S \to \mu^+\mu^-$. Additional Gaussian constraints are applied to the efficiency ratios between $K^0_S \to \mu^+\mu^-$ and $K^0_S \to \pi^+\pi^-$, accounting for the systematic uncertainties. An independent sample of $K^0_S \to \pi^+\pi^-$ decays obtained from a trigger-unbiased sample is used to calibrate the K^0_S invariant mass peak position and resolution parameters (see Fig. 2). It is also used to correct the simulation to obtain the efficiencies of the signal and the normalization channel.

The yield of $K^0 \to \pi^-\mu^+\nu_\mu$ decays as a function of the data taking period is also used to evaluate the variation of the total efficiency with time, mostly caused by changes in the thresholds of the hardware trigger. The obtained single-event sensitivity is $(3.0 \pm 0.6) \times 10^{-12}$, meaning that approximately two $K^0_S \to \mu^+\mu^-$ and five $K^0_L \to \mu^+\mu^-$ signal decays are expected to be present in the data set, using the SM prediction for the branching fractions, and also taking into account the $K^0_L \to \mu^+\mu^-$ detection suppression of 2.3×10^{-3}.

Various sources of systematic uncertainty are taken into account. The main sources are the determination of the trigger efficiency, yielding a systematic uncertainty of 11% for the hardware trigger and 13% for the software trigger; data-simulation differences in the muon identification, with systematic uncertainties varying between 4% and 12%, depending on the trigger category and BDT bin; and the correction applied on simulation, evaluated to be 6%. Other sources, like the efficiency ratio between the signal and normalization modes,

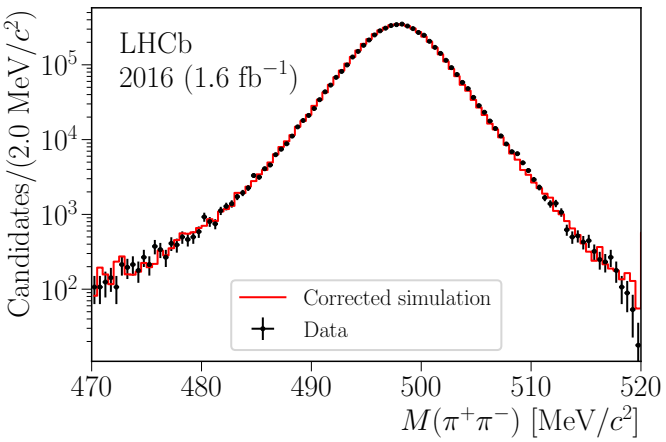

Figure 2: Invariant-mass distribution of $K^0_S \to \pi^+\pi^-$ candidates in 2016 trigger-unbiased data (points with error bars) and corrected simulation (solid histogram). The histogram of simulated candidates is normalized to data.

the BDT response due to changes in the experimental conditions, and the uncertainty on the $K^0_S \to \pi^+\pi^-$ branching fraction are found to be smaller than 5%. The total systematic uncertainty is between 19% and 23%, depending on the trigger category and the BDT bin. It tends to be lower in the TIS trigger category and higher in lower BDT bins, which have lower signal-to-background ratio, due to the stronger muon identification requirements for the lower bins and the bigger systematic uncertainty for the XTOS trigger efficiency. The systematic uncertainties are taken into account as Gaussian constraints in the fit to the data.

The expected significance for a SM signal is 0.1σ, and the expected upper limit is evaluated to be $1.2(1.5)\times10^{-10}$ at 90(95)% C.L. The fit shows no evidence for $K^0_S \to \mu^+\mu^-$ decays (see Fig. 3), with a total yield of 34 ± 23 signal candidates. The signal yield is consistent with zero for all the BDT bins of the two trigger categories. The significance with respect to the background-only hypothesis is 1.5σ (1.4σ when combined with Run 1 data). An upper limit on the branching fraction is obtained by integrating the profile likelihood multiplied by a flat prior in the positive branching fraction domain, yielding $2.2\,(2.6)\times10^{-10}$ at 90(95)% C.L. The likelihood is combined with the Run 1 result, obtaining a limit of $2.1\,(2.4)\times10^{-10}$ at 90(95)% C.L. A log-likelihood interval of one standard deviation ($-2\Delta\log\mathcal{L}=1$) from the Run 2 data set yields $\mathcal{B}(K^0_S\to\mu^+\mu^-) = 1.0^{+0.8}_{-0.7}\times10^{-10}$. Combined with Run 1 it yields $\mathcal{B}(K^0_S\to\mu^+\mu^-) = 0.9^{+0.7}_{-0.6}\times10^{-10}$. The profile likelihoods are shown in Fig. 4.

In summary, a search for the rare decay $K^0_S \to \mu^+\mu^-$ has been performed on a LHCb data set of about $8.6\,\text{fb}^{-1}$. The obtained results supersede those of our previous publications [12, 30]. The data are consistent both with the background-only hypothesis and the combined background and SM signal expectation at the 1.4σ and 1.3σ level, respectively. The most stringent upper limit on the $K^0_S \to \mu^+\mu^-$ branching fraction to date of $2.1\,(2.4)\times10^{-10}$ at 90(95)% confidence level is set, improving the previous best limit by a factor of four.

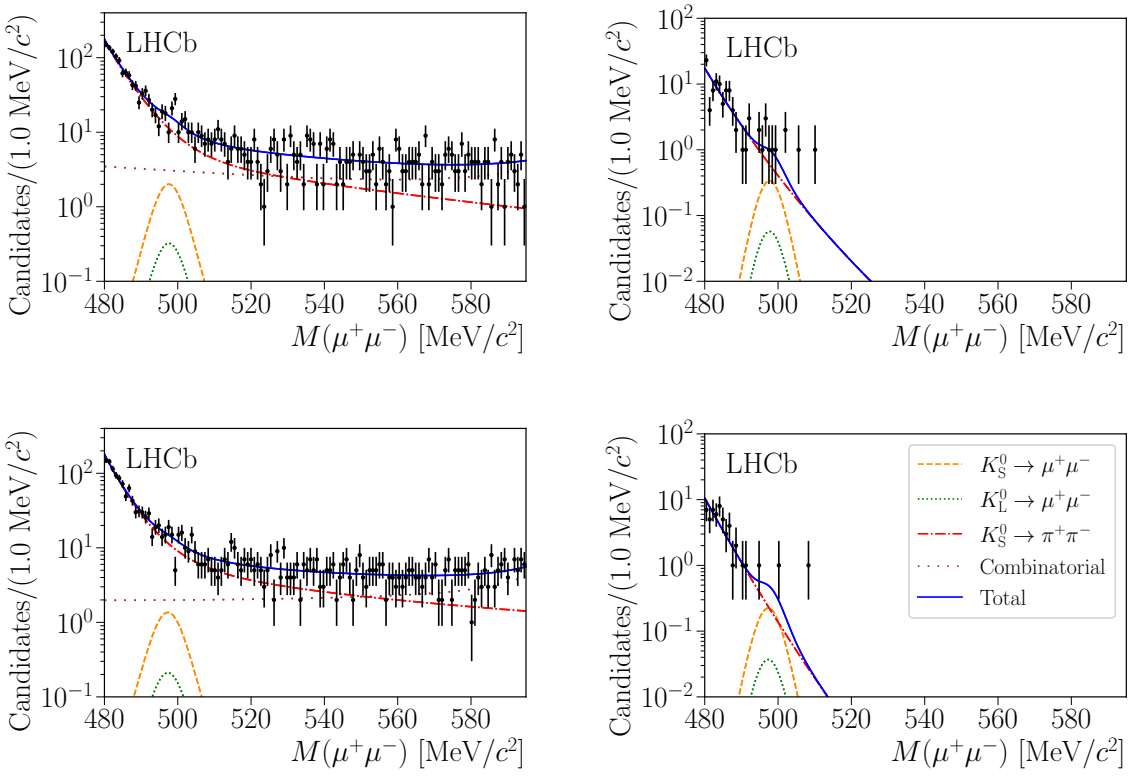

Figure 3: Projection of the fit to the dimuon invariant mass distribution for the (top left) TIS and (bottom left) XTOS trigger categories. The plots on the right correspond to the projection of the fit in the BDT bins with the highest signal-to-background ratio for the (top right) TIS and (bottom right) XTOS trigger categories. The dashed orange line shows the signal contribution, the dotted green line the $K^0_L \to \mu^+\mu^-$ contribution, the dash dotted red line the $K^0_S \to \pi^+\pi^-$ contribution, the loosely dotted brown line the background from random combination of tracks and material interactions, and the solid blue line the total probability density function. For clarity, empty bins are not shown.

Acknowledgements

We would like to thank M. Moulson, J. Martin Camalich, and G. D'Ambrosio for fruitful discussions. We express our gratitude to our colleagues in the CERN accelerator departments for the excellent performance of the LHC. We thank the technical and administrative staff at the LHCb institutes. We acknowledge support from CERN and from the national agencies: CAPES, CNPq, FAPERJ and FINEP (Brazil); MOST and NSFC (China); CNRS/IN2P3 (France); BMBF, DFG and MPG (Germany); INFN (Italy); NWO (Netherlands); MNiSW and NCN (Poland); MEN/IFA (Romania); MSHE (Russia); MinECo (Spain); SNSF and SER (Switzerland); NASU (Ukraine); STFC (United Kingdom); DOE NP and NSF (USA). We acknowledge the computing resources that are provided by CERN, IN2P3 (France), KIT and DESY (Germany), INFN (Italy), SURF (Netherlands), PIC (Spain), GridPP (United Kingdom), RRCKI and Yandex LLC (Russia), CSCS (Switzerland), IFIN-HH (Romania), CBPF (Brazil), PL-GRID (Poland) and OSC (USA). We are indebted to the communities behind the multiple open-source software packages

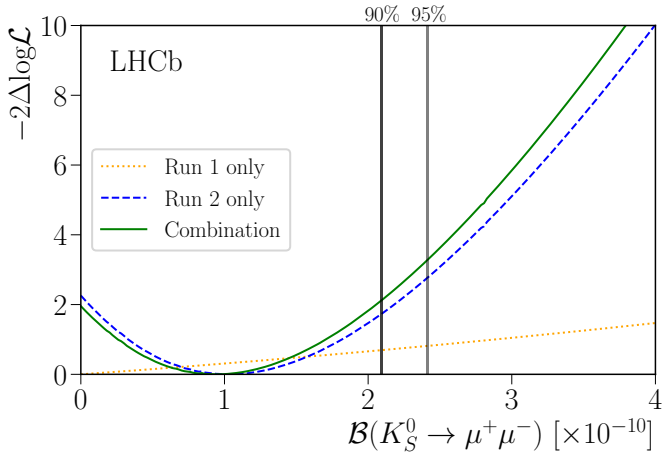

Figure 4: Evaluation of $-2\Delta \log \mathcal{L}$, where $\mathcal{L}$ is the likelihood of the fit model, as a function of $\mathcal{B}(K^0_S \to \mu^+\mu^-)$. The dotted orange line corresponds to the Run 1 result, the dashed blue line to the Run 2 result, and the solid green line shows the combination. The two vertical lines show the location of the upper limit of the combined result at 90% and 95% confidence level.

on which we depend. Individual groups or members have received support from AvH Foundation (Germany); EPLANET, Marie Skłodowska-Curie Actions and ERC (European Union); ANR, Labex P2IO and OCEVU, and Région Auvergne-Rhône-Alpes (France); Key Research Program of Frontier Sciences of CAS, CAS PIFI, and the Thousand Talents Program (China); RFBR, RSF and Yandex LLC (Russia); GVA, XuntaGal and GENCAT (Spain); the Royal Society and the Leverhulme Trust (United Kingdom).

A Supplemental material

In the right sideband of the dimuon invariant mass spectrum, candidates originated from material interactions with the detector dominate, as can be seen in Fig. 5. In order to reduce this contribution, a tool profiting from the parametrization of the VELO using proton-gas events, described in detail in Ref. [27], is used. This algorithm defines an uncertainty-weighted distance to the material

$$D = \sqrt{\left(\frac{x - \mathrm{SV}_x}{\sigma_x}\right)^2 + \left(\frac{y - \mathrm{SV}_y}{\sigma_y}\right)^2 + \left(\frac{z - \mathrm{SV}_z}{\sigma_z}\right)^2},$$

where $\mathrm{SV}_{x,y,z}$ denote the position of the reconstructed secondary vertex in the three coordinates, and $\sigma_{x,y,z}$ the associated uncertainty. This quantity gives information about how likely a vertex arises from an inelastic material interaction.

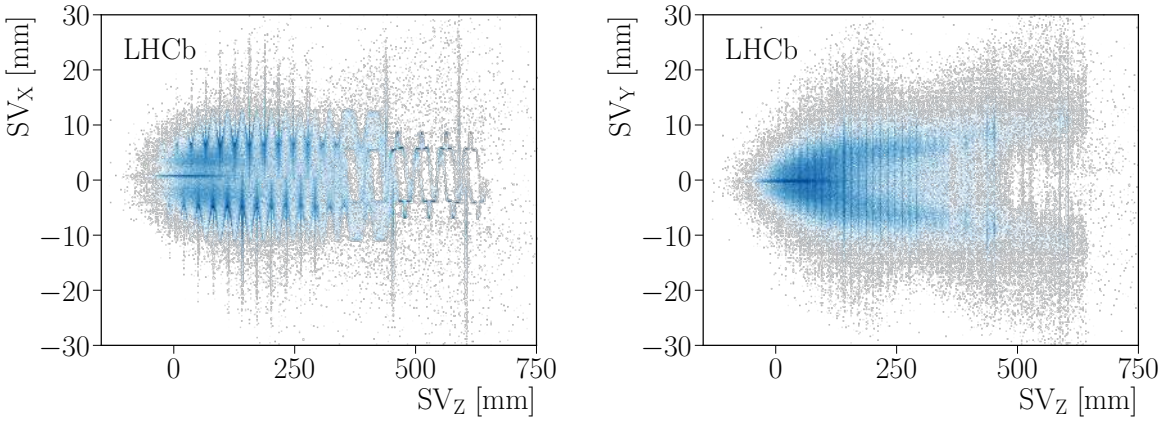

Figure 5: Position of the secondary vertices for $K^0_S \to \mu^+\mu^-$ candidates satisfying the requirement $m_{\mu^+\mu^-} > 520$ MeV/c^2. The pattern of the innermost subdetector of the LHCb, the VELO, can be seen, together with that of the surrounding cavity.

References

[1] G. Ecker and A. Pich, *The longitudinal muon polarization in $K_L \to \mu^+\mu^-$*, Nucl. Phys. **B366** (1991) 189.

[2] G. Isidori and R. Unterdorfer, *On the short distance constraints from $K_{L,S} \to \mu^+\mu^-$*, JHEP **01** (2004) 009, arXiv:hep-ph/0311084.

[3] G. D'Ambrosio and T. Kitahara, *Direct CP violation in $K \to \mu^+\mu^-$*, Phys. Rev. Lett. **119** (2017) 201802, arXiv:1707.06999.

[4] G. D'Ambrosio, G. Ecker, G. Isidori, and H. Neufeld, *Radiative nonleptonic kaon decays*, in *2nd DAPHNE Physics Handbook*, 265, 1994, arXiv:hep-ph/9411439.

[5] Particle Data Group, M. Tanabashi *et al.*, *Review of particle physics*, Phys. Rev. **D98** (2018) 030001.

[6] E871 collaboration, D. Ambrose *et al.*, *Improved branching ratio measurement for the decay* $K^0_{\rm L} \to \mu^+\mu^-$, Phys. Rev. Lett. **84** (2000) 1389.

[7] E137 collaboration, T. Akagi *et al.*, *Experimental study of the rare decays* $K^0_{\rm L} \to \mu e$, $K^0_{\rm L} \to ee$, $K^0_{\rm L} \to \mu\mu$ *and* $K^0_{\rm L} \to eeee$, Phys. Rev. **D51** (1995) 2061.

[8] E791 collaboration, A. Heinson *et al.*, *Measurement of the branching ratio for the rare decay* $K^0_{\rm L} \to \mu^+\mu^-$, Phys. Rev. **D51** (1995) 985.

[9] V. Chobanova *et al.*, *Probing SUSY effects in* $K^0_S \to \mu^+\mu^-$, JHEP **05** (2018) 024, arXiv:1711.11030.

[10] I. Doršner *et al.*, *Limits on scalar leptoquark interactions and consequences for GUTs*, JHEP **11** (2011) 002, arXiv:1107.5393.

[11] C. Bobeth and A. J. Buras, *Leptoquarks meet* ε'/ε *and rare kaon processes*, JHEP **02** (2018) 101, arXiv:1712.01295.

[12] LHCb collaboration, R. Aaij *et al.*, *Improved limit on the branching fraction of the rare decay* $K^0_{\rm S} \to \mu^+\mu^-$, Eur. Phys. J. **C77** (2017) 678, arXiv:1706.00758.

[13] A. A. Alves Jr. *et al.*, *Prospects for measurements with strange hadrons at LHCb*, JHEP **05** (2019) 048, arXiv:1808.03477.

[14] A. A. Alves Jr. *et al.*, *Performance of the LHCb muon system*, JINST **8** (2013) P02022, arXiv:1211.1346.

[15] LHCb collaboration, R. Aaij *et al.*, *LHCb detector performance*, Int. J. Mod. Phys. **A30** (2015) 1530022, arXiv:1412.6352.

[16] R. Aaij *et al.*, *The LHCb trigger and its performance in 2011*, JINST **8** (2013) P04022, arXiv:1211.3055.

[17] F. Dettori, D. Martínez Santos, and J. Prisciandaro, *Low-*$p_{\rm T}$ *dimuon triggers at LHCb in Run 2*, LHCb-PUB-2017-023, 2017.

[18] LHCb collaboration, *Computing Model of the Upgrade LHCb experiment*, CERN-LHCC-2018-014, 2018.

[19] J. A. Hernando Morata *et al.*, *Measurement of trigger efficiencies and biases*, LHCb-2008-073, 2010.

[20] J. Podolanski and R. Armenteros, *Analysis of V-events*, Phil. Mag. **45** (1954) 13.

[21] F. Archilli *et al.*, *Performance of the muon identification at LHCb*, JINST **8** (2013) P10020, arXiv:1306.0249.

[22] Y. Freund and R. E. Schapire, *A decision-theoretic generalization of on-line learning and an application to boosting*, J. Comput. Syst. Sci. **55** (1997) 119.

[23] L. Breiman, J. H. Friedman, R. A. Olshen, and C. J. Stone, *Classification and regression trees*, Wadsworth international group, Belmont, California, USA, 1984.

[24] T. Chen and C. Guestrin, *XGBoost: A scalable tree boosting system*, in *Proceedings of the 22Nd ACM SIGKDD International Conference on Knowledge Discovery and Data Mining*, KDD '16, (New York, NY, USA), 785–794, ACM, 2016, arXiv:1603.02754.

[25] A. Rogozhnikov, *Reweighting with Boosted Decision Trees*, J. Phys. Conf. Ser. **762** (2016) , arXiv:1608.05806, https://github.com/arogozhnikov/hep_ml.

[26] F. Pedregosa *et al.*, *Scikit-learn: Machine learning in Python*, Journal of Machine Learning Research **12** (2011) 2825, see also http://scikit-learn.org.

[27] M. Alexander *et al.*, *Mapping the material in the LHCb vertex locator using secondary hadronic interactions*, JINST **13** (2018) P06008, arXiv:1803.07466.

[28] KLOE-2 collaboration, D. Babusci *et al.*, *Measurement of the branching fraction for the decay $K_S \to \pi\mu\nu$ with the KLOE detector*, arXiv:1912.05990.

[29] D. Martínez Santos and F. Dupertuis, *Mass distributions marginalized over per-event errors*, Nucl. Instrum. Meth. **A764** (2014) 150, arXiv:1312.5000.

[30] LHCb collaboration, R. Aaij *et al.*, *Search for the rare decay $K^0_S \to \mu^+\mu^-$*, JHEP **01** (2013) 090, arXiv:1209.4029.

LHCb collaboration

R. Aaij[31], C. Abellán Beteta[49], T. Ackernley[59], B. Adeva[45], M. Adinolfi[53], H. Afsharnia[9], C.A. Aidala[80], S. Aiola[25], Z. Ajaltouni[9], S. Akar[66], P. Albicocco[22], J. Albrecht[14], F. Alessio[47], M. Alexander[58], A. Alfonso Albero[44], G. Alkhazov[37], P. Alvarez Cartelle[60], A.A. Alves Jr[45], S. Amato[2], Y. Amhis[11], L. An[21], L. Anderlini[21], G. Andreassi[48], M. Andreotti[20], F. Archilli[16], J. Arnau Romeu[10], A. Artamonov[43], M. Artuso[67], K. Arzymatov[41], E. Aslanides[10], M. Atzeni[49], B. Audurier[26], S. Bachmann[16], J.J. Back[55], S. Baker[60], V. Balagura[11,b], W. Baldini[20,47], A. Baranov[41], R.J. Barlow[61], S. Barsuk[11], W. Barter[60], M. Bartolini[23,47,h], F. Baryshnikov[77], G. Bassi[28], V. Batozskaya[35], B. Batsukh[67], A. Battig[14], A. Bay[48], M. Becker[14], F. Bedeschi[28], I. Bediaga[1], A. Beiter[67], L.J. Bel[31], V. Belavin[41], S. Belin[26], N. Beliy[5], V. Bellee[48], K. Belous[43], I. Belyaev[38], G. Bencivenni[22], E. Ben-Haim[12], S. Benson[31], S. Beranek[13], A. Berezhnoy[39], R. Bernet[49], D. Berninghoff[16], H.C. Bernstein[67], C. Bertella[47], E. Bertholet[12], A. Bertolin[27], C. Betancourt[49], F. Betti[19,e], M.O. Bettler[54], Ia. Bezshyiko[49], S. Bhasin[53], J. Bhom[33], M.S. Bieker[14], S. Bifani[52], P. Billoir[12], A. Bizzeti[21,u], M. Bjørn[62], M.P. Blago[47], T. Blake[55], F. Blanc[48], S. Blusk[67], D. Bobulska[58], V. Bocci[30], O. Boente Garcia[45], T. Boettcher[63], A. Boldyrev[78], A. Bondar[42,x], N. Bondar[37], S. Borghi[61,47], M. Borisyak[41], M. Borsato[16], J.T. Borsuk[33], T.J.V. Bowcock[59], C. Bozzi[20], M.J. Bradley[60], S. Braun[16], A. Brea Rodriguez[45], M. Brodski[47], J. Brodzicka[33], A. Brossa Gonzalo[55], D. Brundu[26], E. Buchanan[53], A. Büchler-Germann[49], A. Buonaura[49], C. Burr[47], A. Bursche[26], J.S. Butter[31], J. Buytaert[47], W. Byczynski[47], S. Cadeddu[26], H. Cai[72], R. Calabrese[20,g], L. Calero Diaz[22], S. Cali[22], R. Calladine[52], M. Calvi[24,i], M. Calvo Gomez[44,m], A. Camboni[44,m], P. Campana[22], D.H. Campora Perez[31], L. Capriotti[19,e], A. Carbone[19,e], G. Carboni[29], R. Cardinale[23,h], A. Cardini[26], P. Carniti[24,i], K. Carvalho Akiba[31], A. Casais Vidal[45], G. Casse[59], M. Cattaneo[47], G. Cavallero[47], S. Celani[48], R. Cenci[28,p], J. Cerasoli[10], M.G. Chapman[53], M. Charles[12,47], Ph. Charpentier[47], G. Chatzikonstantinidis[52], M. Chefdeville[8], V. Chekalina[41], C. Chen[3], S. Chen[26], A. Chernov[33], S.-G. Chitic[47], V. Chobanova[45], M. Chrzaszcz[33], A. Chubykin[37], P. Ciambrone[22], M.F. Cicala[55], X. Cid Vidal[45], G. Ciezarek[47], F. Cindolo[19], P.E.L. Clarke[57], M. Clemencic[47], H.V. Cliff[54], J. Closier[47], J.L. Cobbledick[61], V. Coco[47], J.A.B. Coelho[11], J. Cogan[10], E. Cogneras[9], L. Cojocariu[36], P. Collins[47], T. Colombo[47], A. Comerma-Montells[16], A. Contu[26], N. Cooke[52], G. Coombs[58], S. Coquereau[44], G. Corti[47], C.M. Costa Sobral[55], B. Couturier[47], D.C. Craik[63], J. Crkovská[66], A. Crocombe[55], M. Cruz Torres[1,ab], R. Currie[57], C.L. Da Silva[66], E. Dall'Occo[14], J. Dalseno[45,53], C. D'Ambrosio[47], A. Danilina[38], P. d'Argent[16], A. Davis[61], O. De Aguiar Francisco[47], K. De Bruyn[47], S. De Capua[61], M. De Cian[48], J.M. De Miranda[1], L. De Paula[2], M. De Serio[18,d], P. De Simone[22], J.A. de Vries[31], C.T. Dean[66], W. Dean[80], D. Decamp[8], L. Del Buono[12], B. Delaney[54], H.-P. Dembinski[15], M. Demmer[14], A. Dendek[34], V. Denysenko[49], D. Derkach[78], O. Deschamps[9], F. Desse[11], F. Dettori[26,f], B. Dey[7], A. Di Canto[47], P. Di Nezza[22], S. Didenko[77], H. Dijkstra[47], V. Dobishuk[51], F. Dordei[26], M. Dorigo[28,y], A.C. dos Reis[1], L. Douglas[58], A. Dovbnya[50], K. Dreimanis[59], M.W. Dudek[33], L. Dufour[47], G. Dujany[12], P. Durante[47], J.M. Durham[66], D. Dutta[61], M. Dziewiecki[16], A. Dziurda[33], A. Dzyuba[37], S. Easo[56], U. Egede[69], V. Egorychev[38], S. Eidelman[42,x], S. Eisenhardt[57], R. Ekelhof[14], S. Ek-In[48], L. Eklund[58], S. Ely[67], A. Ene[36], E. Epple[66], S. Escher[13], S. Esen[31], T. Evans[47], A. Falabella[19], J. Fan[3], N. Farley[52], S. Farry[59], D. Fazzini[11], P. Fedin[38], M. Féo[47], P. Fernandez Declara[47], A. Fernandez Prieto[45], F. Ferrari[19,e], L. Ferreira Lopes[48], F. Ferreira Rodrigues[2], S. Ferreres Sole[31], M. Ferrillo[49], M. Ferro-Luzzi[47], S. Filippov[40], R.A. Fini[18], M. Fiorini[20,g], M. Firlej[34], K.M. Fischer[62], C. Fitzpatrick[47], T. Fiutowski[34], F. Fleuret[11,b], M. Fontana[47], F. Fontanelli[23,h], R. Forty[47], V. Franco Lima[59], M. Franco Sevilla[65], M. Frank[47], C. Frei[47], D.A. Friday[58], J. Fu[25,q], Q. Fuehring[14], W. Funk[47], E. Gabriel[57], A. Gallas Torreira[45], D. Galli[19,e], S. Gallorini[27], S. Gambetta[57], Y. Gan[3], M. Gandelman[2], P. Gandini[25], Y. Gao[4], L.M. Garcia Martin[46], J. García Pardiñas[49],

B. Garcia Plana[45], F.A. Garcia Rosales[11], J. Garra Tico[54], L. Garrido[44], D. Gascon[44], C. Gaspar[47], D. Gerick[16], E. Gersabeck[61], M. Gersabeck[61], T. Gershon[55], D. Gerstel[10], Ph. Ghez[8], V. Gibson[54], A. Gioventù[45], O.G. Girard[48], P. Gironella Gironell[44], L. Giubega[36], C. Giugliano[20,g], K. Gizdov[57], V.V. Gligorov[12], C. Göbel[70], E. Golobardes[44,m], D. Golubkov[38], A. Golutvin[60,77], A. Gomes[1,a], P. Gorbounov[38,6], I.V. Gorelov[39], C. Gotti[24,i], E. Govorkova[31], J.P. Grabowski[16], R. Graciani Diaz[44], T. Grammatico[12], L.A. Granado Cardoso[47], E. Graugés[44], E. Graverini[48], G. Graziani[21], A. Grecu[36], R. Greim[31], P. Griffith[20,g], L. Grillo[61], L. Gruber[47], B.R. Gruberg Cazon[62], C. Gu[3], P. A. Günther[16], E. Gushchin[40], A. Guth[13], Yu. Guz[43,47], T. Gys[47], T. Hadavizadeh[62], G. Haefeli[48], C. Haen[47], S.C. Haines[54], P.M. Hamilton[65], Q. Han[7], X. Han[16], T.H. Hancock[62], S. Hansmann-Menzemer[16], N. Harnew[62], T. Harrison[59], R. Hart[31], C. Hasse[47], M. Hatch[47], J. He[5], M. Hecker[60], K. Heijhoff[31], K. Heinicke[14], A. Heister[14], A.M. Hennequin[47], K. Hennessy[59], L. Henry[46], J. Heuel[13], A. Hicheur[68], D. Hill[62], M. Hilton[61], P.H. Hopchev[48], J. Hu[16], W. Hu[7], W. Huang[5], W. Hulsbergen[31], T. Humair[60], R.J. Hunter[55], M. Hushchyn[78], D. Hutchcroft[59], D. Hynds[31], P. Ibis[14], M. Idzik[34], P. Ilten[52], A. Inglessi[37], A. Inyakin[43], K. Ivshin[37], R. Jacobsson[47], S. Jakobsen[47], E. Jans[31], B.K. Jashal[46], A. Jawahery[65], V. Jevtic[14], F. Jiang[3], M. John[62], D. Johnson[47], C.R. Jones[54], B. Jost[47], N. Jurik[62], S. Kandybei[50], M. Karacson[47], J.M. Kariuki[53], N. Kazeev[78], M. Kecke[16], F. Keizer[54,47], M. Kelsey[67], M. Kenzie[55], T. Ketel[32], B. Khanji[47], A. Kharisova[79], K.E. Kim[67], T. Kirn[13], V.S. Kirsebom[48], S. Klaver[22], K. Klimaszewski[35], S. Koliiev[51], A. Kondybayeva[77], A. Konoplyannikov[38], P. Kopciewicz[34], R. Kopecna[16], P. Koppenburg[31], M. Korolev[39], I. Kostiuk[31,51], O. Kot[51], S. Kotriakhova[37], L. Kravchuk[40], R.D. Krawczyk[47], M. Kreps[55], F. Kress[60], S. Kretzschmar[13], P. Krokovny[42,x], W. Krupa[34], W. Krzemien[35], W. Kucewicz[33,l], M. Kucharczyk[33], V. Kudryavtsev[42,x], H.S. Kuindersma[31], G.J. Kunde[66], T. Kvaratskheliya[38], D. Lacarrere[47], G. Lafferty[61], A. Lai[26], D. Lancierini[49], J.J. Lane[61], G. Lanfranchi[22], C. Langenbruch[13], O. Lantwin[49], T. Latham[55], F. Lazzari[28,v], C. Lazzeroni[52], R. Le Gac[10], R. Lefèvre[9], A. Leflat[39], O. Leroy[10], T. Lesiak[33], B. Leverington[16], H. Li[71], X. Li[66], Y. Li[6], Z. Li[67], X. Liang[67], R. Lindner[47], V. Lisovskyi[14], G. Liu[71], X. Liu[3], D. Loh[55], A. Loi[26], J. Lomba Castro[45], I. Longstaff[58], J.H. Lopes[2], G. Loustau[49], G.H. Lovell[54], Y. Lu[6], D. Lucchesi[27,o], M. Lucio Martinez[31], Y. Luo[3], A. Lupato[27], E. Luppi[20,g], O. Lupton[55], A. Lusiani[28,t], X. Lyu[5], S. Maccolini[19,e], F. Machefert[11], F. Maciuc[36], V. Macko[48], P. Mackowiak[14], S. Maddrell-Mander[53], L.R. Madhan Mohan[53], O. Maev[37,47], A. Maevskiy[78], D. Maisuzenko[37], M.W. Majewski[34], S. Malde[62], B. Malecki[47], A. Malinin[76], T. Maltsev[42,x], H. Malygina[16], G. Manca[26,f], G. Mancinelli[10], R. Manera Escalero[44], D. Manuzzi[19,e], D. Marangotto[25,q], J. Maratas[9,w], J.F. Marchand[8], U. Marconi[19], S. Mariani[21], C. Marin Benito[11], M. Marinangeli[48], P. Marino[48], J. Marks[16], P.J. Marshall[59], G. Martellotti[30], L. Martinazzoli[47], M. Martinelli[24,i], D. Martinez Santos[45], F. Martinez Vidal[46], A. Massafferri[1], M. Materok[13], R. Matev[47], A. Mathad[49], Z. Mathe[47], V. Matiunin[38], C. Matteuzzi[24], K.R. Mattioli[80], A. Mauri[49], E. Maurice[11,b], M. McCann[60], L. Mcconnell[17], A. McNab[61], R. McNulty[17], J.V. Mead[59], B. Meadows[64], C. Meaux[10], G. Meier[14], N. Meinert[74], D. Melnychuk[35], S. Meloni[24,i], M. Merk[31], A. Merli[25], M. Mikhasenko[47], D.A. Milanes[73], E. Millard[55], M.-N. Minard[8], O. Mineev[38], L. Minzoni[20,g], S.E. Mitchell[57], B. Mitreska[61], D.S. Mitzel[47], A. Mödden[14], A. Mogini[12], R.D. Moise[60], T. Mombächer[14], I.A. Monroy[73], S. Monteil[9], M. Morandin[27], G. Morello[22], M.J. Morello[28,t], J. Moron[34], A.B. Morris[10], A.G. Morris[55], R. Mountain[67], H. Mu[3], F. Muheim[57], M. Mukherjee[7], M. Mulder[31], D. Müller[47], K. Müller[49], V. Müller[14], C.H. Murphy[62], D. Murray[61], P. Muzzetto[26], P. Naik[53], T. Nakada[48], R. Nandakumar[56], A. Nandi[62], T. Nanut[48], I. Nasteva[2], M. Needham[57], N. Neri[25,q], S. Neubert[16], N. Neufeld[47], R. Newcombe[60], T.D. Nguyen[48], C. Nguyen-Mau[48,n], E.M. Niel[11], S. Nieswand[13], N. Nikitin[39], N.S. Nolte[47], C. Nunez[80], A. Oblakowska-Mucha[34], V. Obraztsov[43], S. Ogilvy[58], D.P. O'Hanlon[19], R. Oldeman[26,f], C.J.G. Onderwater[75], J. D. Osborn[80], A. Ossowska[33], J.M. Otalora Goicochea[2], T. Ovsiannikova[38], P. Owen[49],

A. Oyanguren[46], P.R. Pais[48], T. Pajero[28,t], A. Palano[18], M. Palutan[22], G. Panshin[79], A. Papanestis[56], M. Pappagallo[57], L.L. Pappalardo[20,g], C. Pappenheimer[64], W. Parker[65], C. Parkes[61], G. Passaleva[21,47], A. Pastore[18], M. Patel[60], C. Patrignani[19,e], A. Pearce[47], A. Pellegrino[31], M. Pepe Altarelli[47], S. Perazzini[19], D. Pereima[38], P. Perret[9], L. Pescatore[48], K. Petridis[53], A. Petrolini[23,h], A. Petrov[76], S. Petrucci[57], M. Petruzzo[25,q], B. Pietrzyk[8], G. Pietrzyk[48], M. Pili[62], D. Pinci[30], J. Pinzino[47], F. Pisani[47], A. Piucci[16], V. Placinta[36], S. Playfer[57], J. Plews[52], M. Plo Casasus[45], F. Polci[12], M. Poli Lener[22], M. Poliakova[67], A. Poluektov[10], N. Polukhina[77,c], I. Polyakov[67], E. Polycarpo[2], G.J. Pomery[53], S. Ponce[47], A. Popov[43], D. Popov[52], S. Poslavskii[43], K. Prasanth[33], L. Promberger[47], C. Prouve[45], V. Pugatch[51], A. Puig Navarro[49], H. Pullen[62], G. Punzi[28,p], W. Qian[5], J. Qin[5], R. Quagliani[12], B. Quintana[9], N.V. Raab[17], R.I. Rabadan Trejo[10], B. Rachwal[34], J.H. Rademacker[53], M. Rama[28], M. Ramos Pernas[45], M.S. Rangel[2], F. Ratnikov[41,78], G. Raven[32], M. Reboud[8], F. Redi[48], F. Reiss[12], C. Remon Alepuz[46], Z. Ren[3], V. Renaudin[62], S. Ricciardi[56], S. Richards[53], K. Rinnert[59], P. Robbe[11], A. Robert[12], A.B. Rodrigues[48], E. Rodrigues[64], J.A. Rodriguez Lopez[73], M. Roehrken[47], S. Roiser[47], A. Rollings[62], V. Romanovskiy[43], M. Romero Lamas[45], A. Romero Vidal[45], J.D. Roth[80], M. Rotondo[22], M.S. Rudolph[67], T. Ruf[47], J. Ruiz Vidal[46], J. Ryzka[34], J.J. Saborido Silva[45], N. Sagidova[37], B. Saitta[26,f], C. Sanchez Gras[31], C. Sanchez Mayordomo[46], R. Santacesaria[30], C. Santamarina Rios[45], M. Santimaria[22], E. Santovetti[29,j], G. Sarpis[61], A. Sarti[30], C. Satriano[30,s], A. Satta[29], M. Saur[5], D. Savrina[38,39], L.G. Scantlebury Smead[62], S. Schael[13], M. Schellenberg[14], M. Schiller[58], H. Schindler[47], M. Schmelling[15], T. Schmelzer[14], B. Schmidt[47], O. Schneider[48], A. Schopper[47], H.F. Schreiner[64], M. Schubiger[31], S. Schulte[48], M.H. Schune[11], R. Schwemmer[47], B. Sciascia[22], A. Sciubba[30,k], S. Sellam[68], A. Semennikov[38], A. Sergi[52,47], N. Serra[49], J. Serrano[10], L. Sestini[27], A. Seuthe[14], P. Seyfert[47], D.M. Shangase[80], M. Shapkin[43], L. Shchutska[48], T. Shears[59], L. Shekhtman[42,x], V. Shevchenko[76,77], E. Shmanin[77], J.D. Shupperd[67], B.G. Siddi[20], R. Silva Coutinho[49], L. Silva de Oliveira[2], G. Simi[27,o], S. Simone[18,d], I. Skiba[20,g], N. Skidmore[16], T. Skwarnicki[67], M.W. Slater[52], J.G. Smeaton[54], A. Smetkina[38], E. Smith[13], I.T. Smith[57], M. Smith[60], A. Snoch[31], M. Soares[19], L. Soares Lavra[1], M.D. Sokoloff[64], F.J.P. Soler[58], B. Souza De Paula[2], B. Spaan[14], E. Spadaro Norella[25,q], P. Spradlin[58], F. Stagni[47], M. Stahl[64], S. Stahl[47], P. Stefko[48], O. Steinkamp[49], S. Stemmle[16], O. Stenyakin[43], M. Stepanova[37], H. Stevens[14], S. Stone[67], S. Stracka[28], M.E. Stramaglia[48], M. Straticiuc[36], S. Strokov[79], J. Sun[3], L. Sun[72], Y. Sun[65], P. Svihra[61], K. Swientek[34], A. Szabelski[35], T. Szumlak[34], M. Szymanski[5], S. Taneja[61], Z. Tang[3], T. Tekampe[14], G. Tellarini[20], F. Teubert[47], E. Thomas[47], K.A. Thomson[59], M.J. Tilley[60], V. Tisserand[9], S. T'Jampens[8], M. Tobin[6], S. Tolk[47], L. Tomassetti[20,g], D. Tonelli[28], D. Torres Machado[1], D.Y. Tou[12], E. Tournefier[8], M. Traill[58], M.T. Tran[48], C. Trippl[48], A. Trisovic[54], A. Tsaregorodtsev[10], G. Tuci[28,47,p], A. Tully[48], N. Tuning[31], A. Ukleja[35], A. Usachov[11], A. Ustyuzhanin[41,78], U. Uwer[16], A. Vagner[79], V. Vagnoni[19], A. Valassi[47], G. Valenti[19], M. van Beuzekom[31], H. Van Hecke[66], E. van Herwijnen[47], C.B. Van Hulse[17], M. van Veghel[75], R. Vazquez Gomez[44,22], P. Vazquez Regueiro[45], C. Vázquez Sierra[31], S. Vecchi[20], J.J. Velthuis[53], M. Veltri[21,r], A. Venkateswaran[67], M. Vernet[9], M. Veronesi[31], M. Vesterinen[55], J.V. Viana Barbosa[47], D. Vieira[5], M. Vieites Diaz[48], H. Viemann[74], X. Vilasis-Cardona[44,m], A. Vitkovskiy[31], A. Vollhardt[49], D. Vom Bruch[12], A. Vorobyev[37], V. Vorobyev[42,x], N. Voropaev[37], R. Waldi[74], J. Walsh[28], J. Wang[3], J. Wang[72], J. Wang[6], M. Wang[3], Y. Wang[7], Z. Wang[49], D.R. Ward[54], H.M. Wark[59], N.K. Watson[52], D. Websdale[60], A. Weiden[49], C. Weisser[63], B.D.C. Westhenry[53], D.J. White[61], M. Whitehead[13], D. Wiedner[14], G. Wilkinson[62], M. Wilkinson[67], I. Williams[54], M. Williams[63], M.R.J. Williams[61], T. Williams[52], F.F. Wilson[56], W. Wislicki[35], M. Witek[33], L. Witola[16], G. Wormser[11], S.A. Wotton[54], H. Wu[67], K. Wyllie[47], Z. Xiang[5], D. Xiao[7], Y. Xie[7], H. Xing[71], A. Xu[3], L. Xu[3], M. Xu[7], Q. Xu[5], Z. Xu[8], Z. Xu[4], Z. Yang[3], Z. Yang[65], Y. Yao[67], L.E. Yeomans[59], H. Yin[7],

J. Yu[7,aa], X. Yuan[67], O. Yushchenko[43], K.A. Zarebski[52], M. Zavertyaev[15,c], M. Zdybal[33], M. Zeng[3], D. Zhang[7], L. Zhang[3], S. Zhang[3], W.C. Zhang[3,z], Y. Zhang[47], A. Zhelezov[16], Y. Zheng[5], X. Zhou[5], Y. Zhou[5], X. Zhu[3], V. Zhukov[13,39], J.B. Zonneveld[57], S. Zucchelli[19,e].

[1] *Centro Brasileiro de Pesquisas Físicas (CBPF), Rio de Janeiro, Brazil*
[2] *Universidade Federal do Rio de Janeiro (UFRJ), Rio de Janeiro, Brazil*
[3] *Center for High Energy Physics, Tsinghua University, Beijing, China*
[4] *School of Physics State Key Laboratory of Nuclear Physics and Technology, Peking University, Beijing, China*
[5] *University of Chinese Academy of Sciences, Beijing, China*
[6] *Institute Of High Energy Physics (IHEP), Beijing, China*
[7] *Institute of Particle Physics, Central China Normal University, Wuhan, Hubei, China*
[8] *Univ. Grenoble Alpes, Univ. Savoie Mont Blanc, CNRS, IN2P3-LAPP, Annecy, France*
[9] *Université Clermont Auvergne, CNRS/IN2P3, LPC, Clermont-Ferrand, France*
[10] *Aix Marseille Univ, CNRS/IN2P3, CPPM, Marseille, France*
[11] *Université Paris-Saclay, CNRS/IN2P3, IJCLab, Orsay, France*
[12] *LPNHE, Sorbonne Université, Paris Diderot Sorbonne Paris Cité, CNRS/IN2P3, Paris, France*
[13] *I. Physikalisches Institut, RWTH Aachen University, Aachen, Germany*
[14] *Fakultät Physik, Technische Universität Dortmund, Dortmund, Germany*
[15] *Max-Planck-Institut für Kernphysik (MPIK), Heidelberg, Germany*
[16] *Physikalisches Institut, Ruprecht-Karls-Universität Heidelberg, Heidelberg, Germany*
[17] *School of Physics, University College Dublin, Dublin, Ireland*
[18] *INFN Sezione di Bari, Bari, Italy*
[19] *INFN Sezione di Bologna, Bologna, Italy*
[20] *INFN Sezione di Ferrara, Ferrara, Italy*
[21] *INFN Sezione di Firenze, Firenze, Italy*
[22] *INFN Laboratori Nazionali di Frascati, Frascati, Italy*
[23] *INFN Sezione di Genova, Genova, Italy*
[24] *INFN Sezione di Milano-Bicocca, Milano, Italy*
[25] *INFN Sezione di Milano, Milano, Italy*
[26] *INFN Sezione di Cagliari, Monserrato, Italy*
[27] *INFN Sezione di Padova, Padova, Italy*
[28] *INFN Sezione di Pisa, Pisa, Italy*
[29] *INFN Sezione di Roma Tor Vergata, Roma, Italy*
[30] *INFN Sezione di Roma La Sapienza, Roma, Italy*
[31] *Nikhef National Institute for Subatomic Physics, Amsterdam, Netherlands*
[32] *Nikhef National Institute for Subatomic Physics and VU University Amsterdam, Amsterdam, Netherlands*
[33] *Henryk Niewodniczanski Institute of Nuclear Physics Polish Academy of Sciences, Kraków, Poland*
[34] *AGH - University of Science and Technology, Faculty of Physics and Applied Computer Science, Kraków, Poland*
[35] *National Center for Nuclear Research (NCBJ), Warsaw, Poland*
[36] *Horia Hulubei National Institute of Physics and Nuclear Engineering, Bucharest-Magurele, Romania*
[37] *Petersburg Nuclear Physics Institute NRC Kurchatov Institute (PNPI NRC KI), Gatchina, Russia*
[38] *Institute of Theoretical and Experimental Physics NRC Kurchatov Institute (ITEP NRC KI), Moscow, Russia, Moscow, Russia*
[39] *Institute of Nuclear Physics, Moscow State University (SINP MSU), Moscow, Russia*
[40] *Institute for Nuclear Research of the Russian Academy of Sciences (INR RAS), Moscow, Russia*
[41] *Yandex School of Data Analysis, Moscow, Russia*
[42] *Budker Institute of Nuclear Physics (SB RAS), Novosibirsk, Russia*
[43] *Institute for High Energy Physics NRC Kurchatov Institute (IHEP NRC KI), Protvino, Russia, Protvino, Russia*
[44] *ICCUB, Universitat de Barcelona, Barcelona, Spain*
[45] *Instituto Galego de Física de Altas Enerxías (IGFAE), Universidade de Santiago de Compostela, Santiago de Compostela, Spain*
[46] *Instituto de Fisica Corpuscular, Centro Mixto Universidad de Valencia - CSIC, Valencia, Spain*

[47] European Organization for Nuclear Research (CERN), Geneva, Switzerland
[48] Institute of Physics, Ecole Polytechnique Fédérale de Lausanne (EPFL), Lausanne, Switzerland
[49] Physik-Institut, Universität Zürich, Zürich, Switzerland
[50] NSC Kharkiv Institute of Physics and Technology (NSC KIPT), Kharkiv, Ukraine
[51] Institute for Nuclear Research of the National Academy of Sciences (KINR), Kyiv, Ukraine
[52] University of Birmingham, Birmingham, United Kingdom
[53] H.H. Wills Physics Laboratory, University of Bristol, Bristol, United Kingdom
[54] Cavendish Laboratory, University of Cambridge, Cambridge, United Kingdom
[55] Department of Physics, University of Warwick, Coventry, United Kingdom
[56] STFC Rutherford Appleton Laboratory, Didcot, United Kingdom
[57] School of Physics and Astronomy, University of Edinburgh, Edinburgh, United Kingdom
[58] School of Physics and Astronomy, University of Glasgow, Glasgow, United Kingdom
[59] Oliver Lodge Laboratory, University of Liverpool, Liverpool, United Kingdom
[60] Imperial College London, London, United Kingdom
[61] Department of Physics and Astronomy, University of Manchester, Manchester, United Kingdom
[62] Department of Physics, University of Oxford, Oxford, United Kingdom
[63] Massachusetts Institute of Technology, Cambridge, MA, United States
[64] University of Cincinnati, Cincinnati, OH, United States
[65] University of Maryland, College Park, MD, United States
[66] Los Alamos National Laboratory (LANL), Los Alamos, United States
[67] Syracuse University, Syracuse, NY, United States
[68] Laboratory of Mathematical and Subatomic Physics , Constantine, Algeria, associated to [2]
[69] School of Physics and Astronomy, Monash University, Melbourne, Australia, associated to [55]
[70] Pontifícia Universidade Católica do Rio de Janeiro (PUC-Rio), Rio de Janeiro, Brazil, associated to [2]
[71] Guangdong Provencial Key Laboratory of Nuclear Science, Institute of Quantum Matter, South China Normal University, Guangzhou, China, associated to [3]
[72] School of Physics and Technology, Wuhan University, Wuhan, China, associated to [3]
[73] Departamento de Fisica , Universidad Nacional de Colombia, Bogota, Colombia, associated to [12]
[74] Institut für Physik, Universität Rostock, Rostock, Germany, associated to [16]
[75] Van Swinderen Institute, University of Groningen, Groningen, Netherlands, associated to [31]
[76] National Research Centre Kurchatov Institute, Moscow, Russia, associated to [38]
[77] National University of Science and Technology "MISIS", Moscow, Russia, associated to [38]
[78] National Research University Higher School of Economics, Moscow, Russia, associated to [41]
[79] National Research Tomsk Polytechnic University, Tomsk, Russia, associated to [38]
[80] University of Michigan, Ann Arbor, United States, associated to [67]

[a] Universidade Federal do Triângulo Mineiro (UFTM), Uberaba-MG, Brazil
[b] Laboratoire Leprince-Ringuet, Palaiseau, France
[c] P.N. Lebedev Physical Institute, Russian Academy of Science (LPI RAS), Moscow, Russia
[d] Università di Bari, Bari, Italy
[e] Università di Bologna, Bologna, Italy
[f] Università di Cagliari, Cagliari, Italy
[g] Università di Ferrara, Ferrara, Italy
[h] Università di Genova, Genova, Italy
[i] Università di Milano Bicocca, Milano, Italy
[j] Università di Roma Tor Vergata, Roma, Italy
[k] Università di Roma La Sapienza, Roma, Italy
[l] AGH - University of Science and Technology, Faculty of Computer Science, Electronics and Telecommunications, Kraków, Poland
[m] DS4DS, La Salle, Universitat Ramon Llull, Barcelona, Spain
[n] Hanoi University of Science, Hanoi, Vietnam
[o] Università di Padova, Padova, Italy
[p] Università di Pisa, Pisa, Italy
[q] Università degli Studi di Milano, Milano, Italy
[r] Università di Urbino, Urbino, Italy
[s] Università della Basilicata, Potenza, Italy
[t] Scuola Normale Superiore, Pisa, Italy

[u] *Università di Modena e Reggio Emilia, Modena, Italy*
[v] *Università di Siena, Siena, Italy*
[w] *MSU - Iligan Institute of Technology (MSU-IIT), Iligan, Philippines*
[x] *Novosibirsk State University, Novosibirsk, Russia*
[y] *INFN Sezione di Trieste, Trieste, Italy*
[z] *School of Physics and Information Technology, Shaanxi Normal University (SNNU), Xi'an, China*
[aa] *Physics and Micro Electronic College, Hunan University, Changsha City, China*
[ab] *Universidad Nacional Autonoma de Honduras, Tegucigalpa, Honduras*